Journal of Colloid and Interface Science 355 (2011) 472–477

Contents lists available at ScienceDirect

Journal of Colloid and Interface Science

www.elsevier.com/locate/jcis

Size controlled synthesis of Li_2MnSiO_4 nanoparticles: Effect of calcination temperature and carbon content for high performance lithium batteries

V. Aravindan [a,b], S. Ravi [c], W.S. Kim [d], S.Y. Lee [e,*], Y.S. Lee [a,*]

[a] Faculty of Applied Chemical Engineering, Chonnam National University, Gwang-ju 500-757, South Korea
[b] Energy Research Institute, Nanyang Technological University, Research Techno Plaza, 50 Nanyang Drive, Singapore 637553, Singapore
[c] Department of Physics, Mepco Schlenk Engineering College, Sivakasi 626 005, India
[d] Daejung EM Co. Ltd., Incheon 405-820, South Korea
[e] Department of Chemical Engineering, Kangwon National University, Chuncheon 200-701, South Korea

ARTICLE INFO

Article history:
Received 14 July 2010
Accepted 11 December 2010
Available online 16 December 2010

Keywords:
Li_2MnSiO_4 nanoparticles
Adipic acid
EPR
Lithium battery

ABSTRACT

Size controlled, nanoparticulate Li_2MnSiO_4 cathodes were successfully prepared by sol–gel route. Effects of calcination temperature and carbon content (adipic acid) were studied during synthesis process. EPR study was conducted to ensure the formation of phase through oxidation state of manganese. Microscopic pictures indicate spherical shape morphology of the synthesized Li_2MnSiO_4 nanoparticles. Transmission electron microscopic pictures confirmed the presence of carbon coating on the surface of the particles. Further, the optimization has been performed based on phase purity and its battery performance. From the optimization, 700 °C and 0.2 mol adipic acid (against total metal ion present in the compound) were found better conditions to achieve high performance material. The Li_2MnSiO_4 nanoparticles prepared in the aforementioned conditions exhibited an initial discharge capacity of ~113 mAh g^{-1} at room temperature in Li/1 M $LiPF_6$ in EC:DMC/Li_2MnSiO_4 cell configuration. All the Li_2MnSiO_4 nanoparticles prepared at various conditions experienced the capacity fade during cycling.

1. Introduction

In the recent past, 'polyanion' frame work compounds containing tetrahedral 'anion' structural units $(XO_4)^{n-}$ attracted the attention of researchers due to the presence of M–O–X bonds and the possibility of changing the iono-covalent character of the M–O bonding through inductive effect by selecting different X (X = P, Si, As, Mo or W) elements [1]. The selection of transition metal element (X) is crucial to establish tuning the redox potential of the electrodes [2]. The $LiFePO_4$ is one of the commensurate examples for the success story of typical polyanionic framework material, though it exhibited insulating behavior at room temperature [3]. However, conductivity problem has been circumvented by several approaches, among them, introducing the surface coating preferably with carbon is noteworthy [4,5]. Similar to that of phospho olivine groups, lithium rich, orthosilicates, Li_2MSiO_4 (M = Fe, Mn and Co), also fascinated the researchers due to their overwhelming advantages like, high theoretical capacity over 300 mAh g^{-1}, when extracting more than one Li^+ ion per formula unit, high thermal stability through strong Si–O bonding and ease of synthesis [2]. Among the orthosilicate groups Li_2FeSiO_4 and Li_2MnSiO_4 were more attractive than other counterparts since they were cost effective and environmental friendly [6]. Nevertheless, Li_2MnSiO_4 offers higher cell voltage because of the oxidation of Mn^{3+}/Mn^{4+} couple rather than Fe^{2+}/Fe^{3+} in Li_2FeSiO_4. Further, the candidate, Li_2MnSiO_4 was less studied when compared to iron silicate. Similar to that of olivine phosphates, all the members of orthosilicate families were affected due to their inherent conducting behaviors. In the case of olivine $LiFePO_4$, it exhibited superior cell performance after the introduction of carbon coating [4,5]. A similar procedure shall help to overcome the conductivity issues associated with orthosilicate groups.

So far, very few reports could be traced for the synthesis and characterization of Li_2MnSiO_4 either through solid state or sol–gel route [6–19]. These two routes are appropriate procedures for mass production in industries. Further, Sol–gel route is convenient when compared to solid state approaches, in its capacity to synthesize the desired particulate morphologies having good stoichiometry. Earlier, Jamnic et al. [9] reported the synthesis and performance of Li_2MnSiO_4 by modified Pechni sol–gel route. In this process, SiO_2 is dispersed in water and Mn and Li Source materials were added to form gel and finally heat treated to yield the resultant product. But, in such process a real solution phase reaction does not take place, which is also similar to that of solid state reaction. Li et al. [18] also reported the solution phase sol–gel route by using tetraethoxysilane as source material for silicon. However,

* Corresponding authors. Fax: +82 62 530 1909 (Y.S. Lee).
E-mail addresses: aravind_van@yahoo.com (V. Aravindan), leeys@chonnam.ac.kr (Y.S. Lee).

0021-9797/$ - see front matter © 2010 Elsevier Inc. All rights reserved.
doi:10.1016/j.jcis.2010.12.038

authors presented without any optimization which provides poor cell performance having lots of impurity phases. Recently, Belharouak et al. [16] reported the sol–gel synthesized Li_2MnSiO_4, but failed to control the morphologies, which leads to aggregation of the resultant material. Further, ball milling was employed for the carbon coating after the aggregation takes place, which in turn provides the heterogeneous coating. In this connection, an attempt has been made to control the morphology through optimizing the temperature and carbon coating (*in situ*) in real solution phase reaction by sol–gel route to effectively improve the performance of the cell.

2. Materials and methods

Li_2MnSiO_4 nanoparticles were synthesized from the source materials of $LiCH_3COO$ (Sigma–Aldrich, USA), $Si(CH_3COO)_4$ (Sigma–Aldrich, USA), $Mn(CH_3COO)_2$ (Sigma–Aldrich, USA), and $C_6H_{10}O_4$ (Sigma–Aldrich, USA) using sol–gel method. A stoichiometric amount of each material were dissolved in ethanol and mixed well with an aqueous solution of adipic acid with various concentrations ranging from 0 to 1 mol against total metal ions present in Li_2MnSiO_4. The solution was evaporated at 90 °C to form transparent solution (sol). Then, the sol was transferred to vacuum oven and dried at 90–100 °C to obtain the gel precursors. Resulted precursor was finely ground and calcined at various temperature conditions with 50 °C interval for 5 h in Ar atmosphere. Structural properties were studied by Powder X-ray diffraction (XRD, Rint 1000, Rigaku, Japan) using Cu Kα radiation. Thermal studies were carried out by means of thermogravimetric-differential thermal analysis (TG-DTA) using a thermal analyzer system (STA 1640, Stanton Redcroft Inc., UK). A thin Pt plate was used as the sample holder. The powder was heated at 5 °C/min and cooled at 10 °C/min. The surface morphological features of the resulting compounds were observed using a field emission scanning electron microscope (FE-SEM, S-4700, Hitachi, Japan). The high resolution-transmission electronic microscopy (HR-TEM, TECNAI, Philips, Netherlands) is utilized to study the carbon coating on the surface of Li_2MnSiO_4. The cathode was fabricated with 20 mg of accurately weighed active material, 3 mg of Ketzen black and 3 mg of conductive binder (Teflonized acetylene black (TAB)). It was pressed on a 200 mm^2 stainless steel mesh which was used as the current collector under a pressure of 300 kg/cm^2 and dried at 130 °C for 5 h in an oven. The cell was made of a cathode and metallic lithium as anode, which were separated by a porous polypropylene film (Celgard 3401). The mixture of 1 M $LiPF_6$-ethylene carbonate (EC)/dimethyl carbonate (DMC) (1:1 v/v, Techno Semichem Co., Ltd., Korea) was used as electrolyte. The galvanostatic cycling studies were conducted in the two electrode configuration using CR 2032 coin cell between 1.5 and 4.8 V at 0.05 C in room temperature conditions.

3. Results and discussion

Thermogravimetric-derivative thermal analysis (TG-DTA) was used to establish the temperature conditions for the synthesis of Li_2MnSiO_4 nanoparticles. Fig. 1 shows the TG traces, performed on the Li_2MnSiO_4 source materials with adipic acid (0.1 mol). It is apparent to notice that, the thermogram is clearly separated by two main stages of thermal events. The first stage of endothermic events starts at ~50 °C and it showed a gradual weight loss up to ~300 °C. These initial weight losses are recognized to the dehydration and decomposition of acetate groups from the starting materials, as well as to the inclusion of gelating agent (carbon source) *i.e.* adipic acid melting. The second thermal event with sharp endotherm (~43% weight loss) at ~300–430 °C, which can be predictable by the decomposition of remaining reactants from

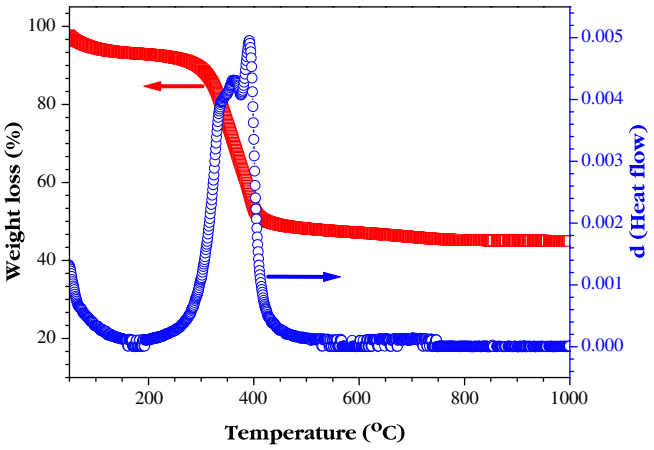

Fig. 1. Thermogravimetric traces of starting materials for synthesis of Li_2MnSiO_4 in an Ar atmosphere.

the source materials as well as the carbonization of adipic acid. Thereafter, no noticeable thermal events were observed, which confirm the formation of single phase Li_2MnSiO_4 nanoparticles (>430 °C). The derivative curve also reflects the weight loss observed in TG analysis around 300–400 °C. A series of compounds were prepared from 600 °C to 800 °C with the interval of 50 °C in order to optimize the temperature condition for the synthesis of Li_2MnSiO_4 phase.

Fig. 2 represents the series of powder X-ray diffraction patterns of synthesized Li_2MnSiO_4 with various temperatures. The XRD reflections showed a well defined sharp intense satellite peaks, which indicates the crystalline nature of Li_2MnSiO_4 prepared at various temperature conditions. Further, there are no reflections, which indicate the appearance of the starting materials used for the synthesis. The Li_2MnSiO_4 can be isostructural to certain forms of Li_3PO_4: Mn^{2+} ions are present within a $[SiO_4]$ anionic silicate network that replaces $[PO_4]$ anionic phosphate network, and two Li ions are available in 3D dimensional channels. Further, we believe that the strong Si–O bonds may translate good electrochemical and thermal properties for safety issues. The temperature optimization is performed in the presence of 0.1 mol adipic acid as gelating agent. It is apparent to notice that, all the observed patterns with interval of 50 °C from 600 °C to 800 °C having impurity phases MnO, Mn_2SiO_4 or Li_2SiO_3 along with Li_2MnSiO_4 phase. Consequently, the material prepared at 700 °C showed the absence of

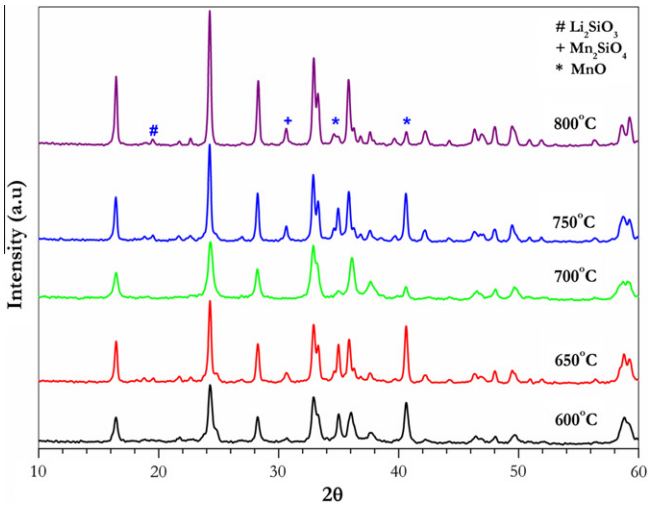

Fig. 2. Powder X-ray diffraction patterns of synthesized Li_2MnSiO_4 nanoparticles at various temperatures in Ar atmosphere.

Mn_2SiO_4 phase. The trace amount of MnO is unavoidable, which is observed all the prepared materials having appreciable amount. The presence of impurity phases during the synthesis of Li_2MnSiO_4 is also noticed other researchers by various routes [6,8–17]. For example, de Dompablo et al. [15] succeeded to prepare Li_2MnSiO_4 material in the absence of MnO phase by varying the pressure, but in the formation of Mn_2SiO_4 could be inevitable under such abnormal pressure conditions. In addition to that, the presence of Mn_2SiO_4 phase is much prevailing than those of MnO presence in the conventional synthesis either solid state or sol–gel. The obtained XRD pattern of Li_2MnSiO_4 nanoparticles reveal the purest pattern reported elsewhere, even though containing some impurities [16]. In order to confirm the purity of the pattern observed from this synthesis, spectroscopic tools (EPR) were used to verify the nature of Li_2MnSiO_4 phase through the oxidation state of manganese (will be discussed later). From this study and based on the previous reports it has been confirmed that the preparation of 100% phase pure Li_2MnSiO_4 is complicated. All the phases prepared at various temperature conditions contained at least any one of the impurities, hence, the optimization of the temperature was performed based on battery performance of the material. Accordingly, the cells, Li/Li_2MnSiO_4 were assembled and the battery performance was evaluated at room temperature as given in Fig. 3. The Li_2MnSiO_4 prepared at 700 °C exhibited the initial discharge capacity of 102 mAh g^{-1} and rest of Li_2MnSiO_4 phase materials exhibited

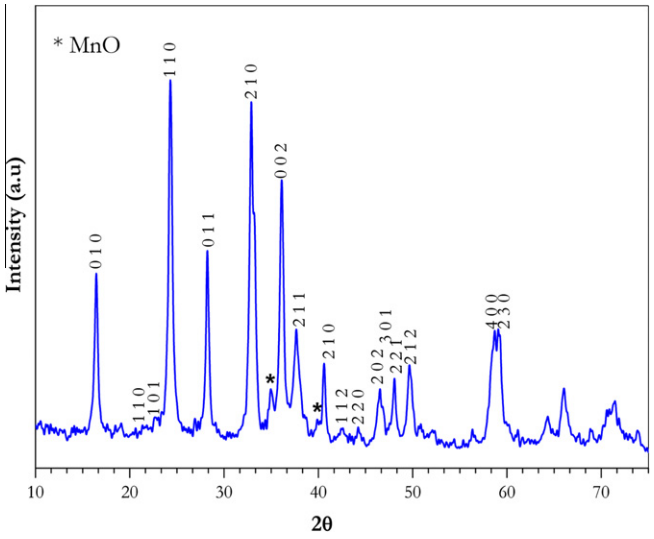

Fig. 4. Powder X-ray diffraction patterns of synthesized Li_2MnSiO_4 nanoparticles at 700 °C with 0.2 mol adipic acid concentration.

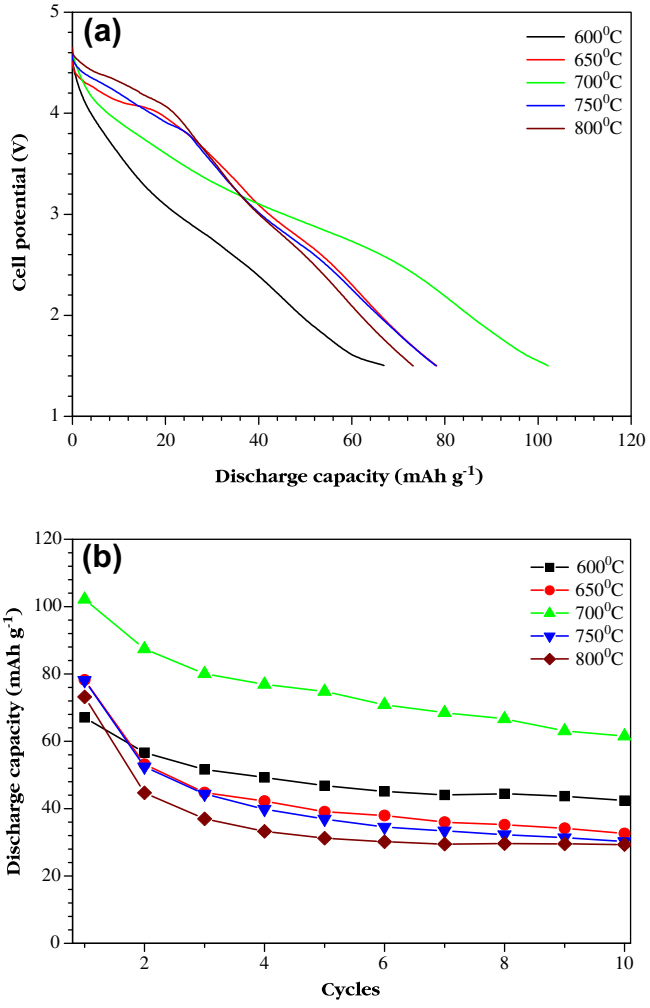

Fig. 3. The cell performance of Li_2MnSiO_4 nanoparticles prepared by various temperatures (a) discharge capacity profiles and (b) corresponding cycling performance of Li/Li_2MnSiO_4 cells at ambient temperatures.

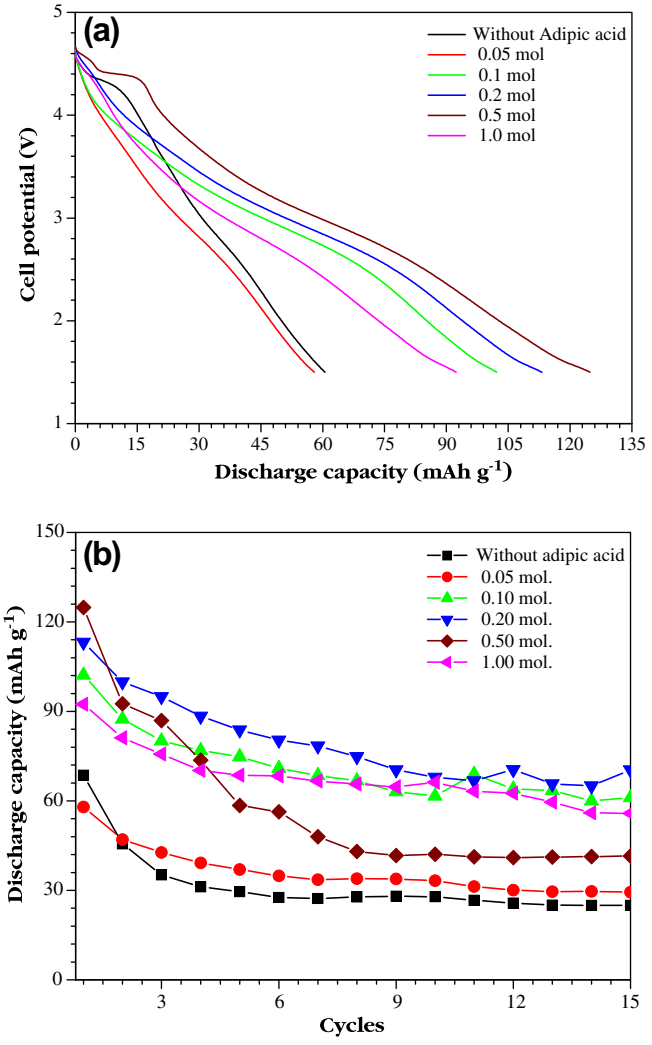

Fig. 5. The cell performance of Li_2MnSiO_4 nanoparticles prepared at 700 °C with various adipic acid concentrations (a) discharge capacity profiles and (b) corresponding cycling performance of Li/Li_2MnSiO_4 cells at ambient temperatures.

the initial discharge capacity under 80 mAh g^{-1}. The drastic variation of the capacity profile may be attributed to the presence of inactive Mn_2SiO_4 moieties. From the optimization, a temperature of 700 °C is found to be the better optimal condition to accomplish high performance Li_2MnSiO_4 nanoparticles. The orthosilicate materials suffered by inherent conducting properties (Li_2FeSiO_4 = $\sim 2 \times 10^{-12}$ S cm^{-2} and Li_2MnSiO_4 = $\sim 3 \times 10^{-14}$ S cm^{-2}) at ambient temperature conditions [10]. The electronic conductivities of iron or manganese silicates were three to five orders of magnitudes lower than $LiFePO_4$ ($\sim 10^{-9}$ S cm^{-2}). Hence, the strong conductive coating preferably, carbon coating is required to improve the electronic conductivity of the orthosilicate materials. At the same time, reduction in the particle size (nanometric range) is also one of the important phenomena for the faster diffusion of lithium ions during cycling process. Generally, carbon coating were employed by two different approaches, (i) the desired phase material was prepared by either solid state or sol–gel and later the conducting carbon was added and milled with optimized conditions (*ex situ*) and (ii) the source material of carbon was included during the synthesis and fired in an inert atmosphere at high temperature providing the carbon coating along with original phase material (*in situ*). Among the two routes, milling with carbon resulted in heterogeneous coating and also required an additional heat treatment, whereas in the later case very simple and homogeneous coating could be obtained. Further, the choice of carbon source material is also an important factor; it should be carbon rich and effectively control the aggregation during the calcination process, like carboxylic acids [20]. The purpose of using gelating agent, particularly carboxylic (–COOH–) functional group containing materials, which act as capping agent as well as carbon source material to prevent aggregation during synthesis. Among the carboxylic acids, the adipic acid is one of the best sources of carbon and as well as gelating agent for the preparation of materials through either solid state or sol–gel route. This was convincingly proven by our previous work on $LiFePO_4$ by solid state as well as sol–gel [21,22]. In order to satisfy the aforementioned requirements gelating agent or carbon source (adipic acid) concentration was varied during the synthesis process from 0 to 1.0 mol against the total metal ion present in the Li_2MnSiO_4 at 700 °C.

Fig. 4 illustrates the X-ray diffractogram of Li_2MnSiO_4 prepared at 700 °C with the adipic acid concentration of 0.2 mol. All the materials prepared at different concentrations exhibited the same pattern containing little amount of MnO impurities (only 0.2 mol adipic acid comprising material was presented). The observed reflections were indexed according to the orthorhombic structure (Li_2MnSiO_4 having Li_3PO_4 structure.) with $Pmn2_1$ space group [16]. Similar to that of temperature optimization, the adipic acid concentration also optimized based on the cell performance of the materials. In this connection, all the materials tested in Li/Li_2MnSiO_4 configuration in the presence of 1 M $LiPF_6$ in EC:DMC electrolyte are given in Fig. 5. The cells presented the initial discharge capacity of 125, 113, 102, 92, 68 and 58 mAh g^{-1} for 0.5, 0.2, 0.1, 1.0, 0 and 0.05 mol adipic acid concentration respectively, against the total metal ion present in the Li_2MnSiO_4. The high concentration of adipic acid comprising compounds exhibited a good discharge capacity profile, say beyond 0.1 mol, whereas in the case of less adipic acid containing materials (0.05 mol) and those without adipic acid materials exhibited poor capacity. The reason for improvement in the capacity profile may be attributed to the improved electronic conductivity of the materials via the carbonization of adipic acid during the calcination process. The carbonization of gelating agent may form the thin layer of carbon on the surface of the Li_2MnSiO_4 particles providing the improvement in electronic conductivity [21,22]. However, the adipic acid concentration increases beyond 0.2 mol also approaching the poor capacity profile. The 0.2 mol adipic acid treated Li_2MnSiO_4 particles comprising 0.92 wt.% carbon in the final stage, which was confirmed by CHN analysis. This may be due to the high carbon content, which leads to the dilution of active material distance resulting in suppression of discharge capacity results poor capacity

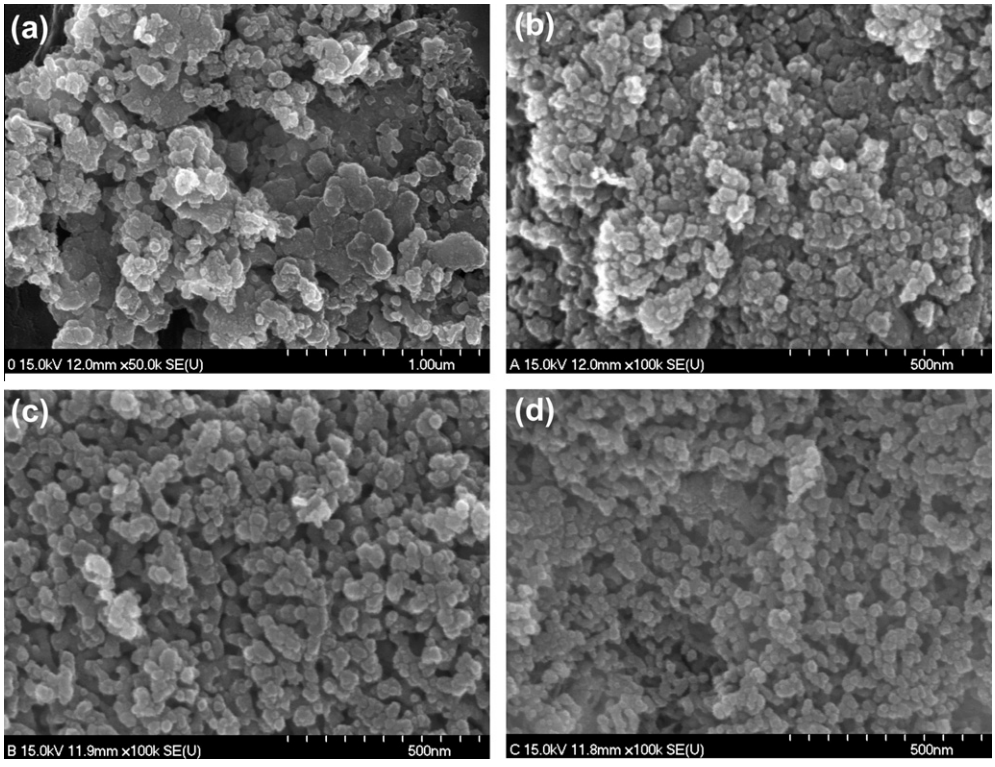

Fig. 6. Scanning electron microscopic pictures of Li_2MnSiO_4 nanoparticles containing various adipic acid concentrations (a) 0 mol, (b) 0.05 mol, (c) 0.1 mol and (d) 0.2 mol.

profile. The case of Li_2MnSiO_4 containing less amount of adipic acid does not show noticeable improvement in the capacity profile, which may be due to the concentration which is not sufficient for the improvement in electronic conductivity [22]. It is apparent to notice that, all the cells were experiencing the capacity fading during the cycling. This may be attributed to the destruction of crystal structure during the cycling process which leads to the amorphous state [18]. It is surprising to see that, when increasing the carbon content hampering the crystal structure destruction. Further detailed *in situ*-XRD investigations and altering the compositions of the electrodes are in progress to achieve the good electrochemical stability during cycling. Based on the studies of 0.2 mol adipic acid prepared at 700 °C in Ar atmosphere could be the optimal concentration to attain the high performance material.

Morphological features of the Li_2MnSiO_4 (optimization of adipic acid) nanoparticles, 0, 0.05, 0.1 and 0.2 mol adipic acid concentrations are given in Fig. 6. It is obvious to notice that, adipic acid free Li_2MnSiO_4 materials exhibited highly aggregated lump like particulate morphology. When increasing the concentration of adipic acid to 0.05 mol, the aggregation of the particles tends to get reduced due to the presence of adipic acid. As a consequence, the adipic acid concentration is not sufficient to prevent the aggregation completely. So, again increasing the concentration to 0.1 mol, the particles are exhibiting good spherical morphology with little aggregation of the particles having the size around 50 nm. However, still the adipic acid concentration is not strong enough to control the aggregation fully. Li_2MnSiO_4 comprising 0.2 mol adipic acid exhibited highly monodispersed spherical shape morphology with particle size around ~25–30 nm. From the SEM pictures, it is obvious that increasing the adipic acid concentration leads to the prevention of aggregation and formation of highly monodispersed Li_2MnSiO_4 nanoparticles.

Fig. 7 illustrates the transmission electron microscopic images of 0.2 mol adpic acid treated Li_2MnSiO_4 nanoparticles prepared through sol–gel route. The pictures clearly indicate the appearance of weakly aggregated nanoparticulates with sizes less than 50 nm. The HR-TEM image (Fig. 7b) confirmed the presence of almost homogeneous carbon layer on the surface of Li_2MnSiO_4 nanoparticles. This TEM reveals the effective use of gelating agent during synthesis process which prevents particles growth at solution phase reaction. Thereafter, during high temperature sintering at inert atmosphere, the adipic acid was carbonized and form as carbon on the surface, which prevents the growth of particles as well as enhances the electronic conductivity of the material.

The obtained phase was confirmed by electron paramagnetic resonance (EPR) due to the presence of Mn (II) with full range is given in Fig. 8. The EPR traces were recorded for Li_2MnSiO_4 material

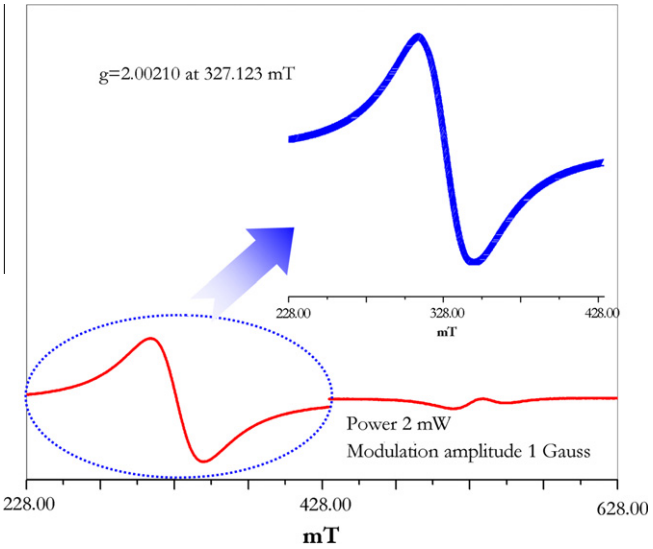

Fig. 8. Electron paramagnetic resonance (EPR) curves of Li_2MnSiO_4 recorded at room temperature with the power of 2 mW and modulation of amplitude of 1 gauss.

containing 0.1 mol adipic acid. The Mn (II) also exhibits the weak signal around 528.00 mT, however the signal is too weak to analyze. So, the strong signal around 328.00 mT is taken into account for the calculation of g factor. The EPR is an excellent tool to localize the state of any paramagnetic element present in the host. Manganese is occurs in nature with various oxidation states (+1 to +6) depending on charge compensation with the ligands. Since it is divalent ion, it quickly tries to enter the compound in 2+ oxidation states but sometimes this may change due to the surrounding environment and symmetry. Since it is purely based on spin, the results give accurate and non speculative information regarding the nature and details of an element which possess net spin. As we know manganese exhibit in 2+ oxidation state readily, it gives 30 hyperfine lines in EPR spectrum (spin S = 5/2 and I = 5/2) with 6 main hyperfine lines (if it sits in perfect cubic symmetry) and each main hyperfine line comprises of 5 lines which may sometime become difficult to resolve. Fig. 8 shows single broad line centered as $g = 2.00$ which indicates the existence of Mn^{2+} state. It appears that it is a sufficient lattice disorder to introduce ill-defined lower symmetry crystal field which broadens and eliminates other observability except $M_S = +1/2 \leftrightarrow M_S = -1/2$ transition. This was proven in many spinal based systems since the oxygen

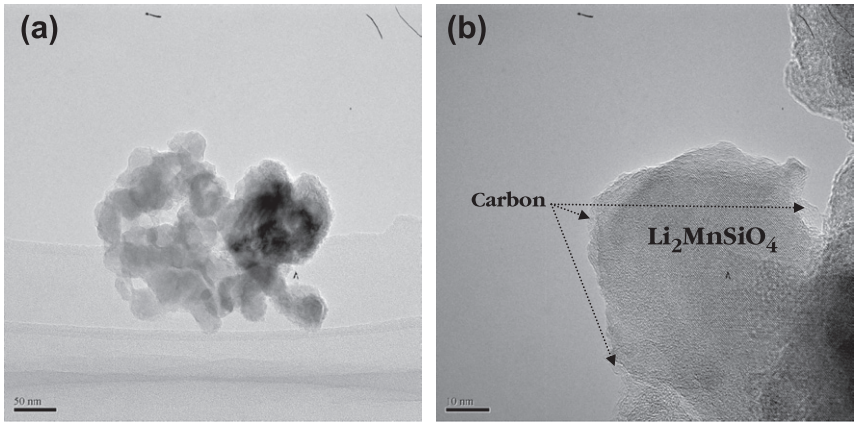

Fig. 7. (a) Transmission electron microscopic image of Li_2MnSiO_4 nanoparticles containing 0.2 mol adipic acid and (b) high resolution-transmission electron microscopic pictures indicates the presence of carbon layer on the surface.

bond surrounding manganese is difficult to study [23,24]. In our present study, manganese exhibited perfect cubic symmetry with single broad peak centered at $g \cong 2.0$ which is a good fit for Mn^{2+} in cubic symmetry. Thus it is reasonable to assume that manganese is present in our system in 2+ oxidation state. This confirms the observed pattern having excellent phase purity though adipic acid accosted sol–gel process.

4. Conclusion

The Li_2MnSiO_4 nanoparticles were succesfully synthesized by sol–gel route with highest purity. The effect of calcination temperature and carbon content (adipic acid) were optimized based on the phase purity as well as battery performance. The phase purity has been confirmed by electron paramagnetic resonance spectroscopy via the oxidation state of Mn (II) ions. Results of our current efforts revealed that, 0.2 mol adipic acid at 700 °C could be the optimum concentration to prepare good performance material. Based on the aforementioned conditions, the prepared Li_2MnSiO_4 nanoparticles presented the initial discharge capacity of 113 mAh g^{-1} at room temperature. However all the cells experienced the capacity fade during cycling, hence further studies are in progress to alliviate that issue.

Acknowledgment

This work was supported by the grant from the Technology Innovation Program of the Ministry of Knowledge Economy of Korea (Project No. K1002176).

References

[1] S.Y. Chung, J.T. Bloking, Y.-M. Chiang, Nat. Mater. 1 (2002) 123–128.
[2] M.E.A. de Dompablo, M. Armand, J.M. Tarascon, U. Amador, Electrochem. Commun. 8 (2006) 1292–1298.
[3] A.K. Padhi, K.S. Nanjundaswamy, J.B. Goodenough, J. Electrochem. Soc. 144 (1997) 1188–1194.
[4] Z. Li, D. Zhang, F. Yang, J. Mater. Sci. 44 (2009) 2435–2443.
[5] D. Jugovic, D. Uskokovic, J. Power Sour. 190 (2009) 538–544.
[6] C. Deng, S. Zhang, B.L. Fu, S.Y. Yang, L. Ma, Mater. Chem. Phys. 120 (2010) 14–17.
[7] K. Karthikeyan, V. Aravindan, S.B. Lee, I.C. Jang, H.H. Lim, G.J. Park, M. Yoshio, Y.S. Lee, J. Alloys Compd. 504 (2010) 224–227.
[8] A. Nytén, A. Abouimrane, M. Armand, T. Gustafsson, J.O. Thomas, Electrochem. Commun. 7 (2005) 156–160.
[9] R. Dominko, M. Bele, M. Gaberšček, A. Meden, M. Remškar, J. Jamnik, Electrochem. Commun. 8 (2006) 217–222.
[10] A. Kokalj, R. Dominko, G. Mali, A. Meden, M. Gaberscek, J. Jamnik, Chem. Mater. 19 (2007) 3633–3640.
[11] R. Dominko, J. Power Sour. 184 (2008) 462–468.
[12] W. Liu, Y. Xu, R. Yang, J. Alloys Compd. 480 (2009) L1–L4.
[13] K. Karthikeyan, V. Aravindan, S.B. Lee, I.C. Jang, H.H. Lim, G.J. Park, M. Yoshio, Y.S. Lee, J. Power Sour. 195 (2010) 3761–3764.
[14] R. Dominko, I. Arcon, A. Kodre, D. Hanzel, M. Gaberscek, J. Power Sour. 189 (2009) 51–58.
[15] M.E.A. de Dompablo, R. Dominko, J.M.G. Amores, L. Dupont, G. Mali, H. Ehrenberg, J. Jamnik, E. Moran, Chem. Mater. 20 (2008) 5574–5584.
[16] I. Belharouak, A. Abouimrane, K. Amine, J. Phys. Chem. C 113 (2009) 20733–20737.
[17] V. Aravindan, K. Karthikeyan, S. Ravi, S. Amaresh, W.S. Kim, Y.S. Lee, J. Mater. Chem. 20 (2010) 7340–7343.
[18] Y.X. Li, Z.L. Gong, Y. Yang, J. Power Sour. 174 (2007) 528–532.
[19] R. Dominko, M. Bele, A. Kokalj, M. Gaberscek, J. Jamnik, J. Power Sour. 174 (2007) 457–461.
[20] G.T.K. Fey, T.L. Lu, F.Y. Wu, W.H. Li, J. Solid State Electrochem. 12 (2008) 825–833.
[21] H.H. Lim, I.C. Jang, S.B. Lee, K. Karthikeyan, V. Aravindan, Y.S. Lee, J. Alloys Compd. 495 (2010) 181–184.
[22] S.B. Lee, I.C. Jang, H.H. Lim, V. Aravindan, H.S. Kim, Y.S. Lee, J. Alloys Compd. 491 (2010) 668–672.
[23] L. Pawlak, K. Falkowski, S. Pokrzywnicki, J. Solid State Chem. 37 (1991) 228–231.
[24] A. Abraham, B. Bleaney, Electron Paramagnetic Resonance of Transition Ions, Oxford University Press, 1970. p. 447.